CHIN. PHYS. LETT. Vol. 35, No. 5 (2018) 050301

Dynamical Evolution of an Effective Two-Level System with $\mathcal{PT}$ Symmetry *

Lei Du(杜磊)[1], Zhihao Xu(徐志浩)[1,2,3], Chuanhao Yin(尹传昊)[4], Liping Guo(郭利平)[1,2,3]**

[1]*Institute of Theoretical Physics, Shanxi University, Taiyuan 030006*
[2]*Collaborative Innovation Center of Extreme Optics, Shanxi University, Taiyuan 030006*
[3]*State Key Laboratory of Quantum Optics and Quantum Optics Devices, Institute of Opto-Electronics, Shanxi University, Taiyuan 030006*
[4]*Institute of Physics, Chinese Academy of Sciences, Beijing 100190*

(Received 27 December 2017)

We investigate the dynamics of parity- and time-reversal ($\mathcal{PT}$) symmetric two-energy-level atoms in the presence of two optical and one radio-frequency fields. The strength and relative phase of fields can drive the system from the unbroken to the broken $\mathcal{PT}$ symmetric regions. Compared with the Hermitian model, Rabi-type oscillation is still observed, and the oscillation characteristics are also adjusted by the strength and relative phase in the region of the unbroken $\mathcal{PT}$ symmetry. At the exception point, the oscillation breaks down. To better understand the underlying properties we study the effective Bloch dynamics and find that the emergence of the z components of the fixed points is the feature of the $\mathcal{PT}$ symmetry breaking and the projections in the x–y plane can be controlled with high flexibility compared with the standard two-level system with the $\mathcal{PT}$ symmetry. It helps to study the dynamic behavior of the complex $\mathcal{PT}$ symmetric model.

PACS: 03.65.Yz, 03.75.Kk, 03.65.−w DOI: 10.1088/0256-307X/35/5/050301

In the past few decades non-Hermitian Hamiltonians describing open physical systems have attracted increasing research interest, with particular attention paid to a class of $\mathcal{PT}$ symmetric Hamiltonians where the spectrum might be completely real-valued.[1] A surge of work has been devoted to their experimental implementation in diverse physical systems, ranging from optical waveguide structures,[2,3] flat microwave cavities[4] and optical cavities,[5–8] electronic circuits[9] and whispering-gallery modes[10] to mesh lattices.[11] The relevant properties of $\mathcal{PT}$ symmetric Hamiltonians have been extensively studied, such as eigenvalues, eigenfunctions and dynamical evolution. Among all of $\mathcal{PT}$ symmetric systems, a model of two coupled modes subjected to gain and loss with equal amplitudes is of particular interest, because it is the minimal system to reveal $\mathcal{PT}$ physics.[12–16] The extension of two such modes to many modes with $\mathcal{PT}$ symmetry also exists, such as the so-called Bose–Hubbard dimer[17–19] and a one-dimensional tight-binding chain with two conjugated imaginary potentials at two edges.[20]

In experiments, a two-level atom coupled with a near resonant radiation field can describe a coupled two-mode system. The coupling between two levels can also be implemented in many ways, e.g., two coupled hyperfine levels can be produced by adiabatically eliminating the third intermediate level using Raman lasers in a Λ-type three-level atomic system.[21–23] The two hyperfine energy levels can be directly dressed by a microwave field or an rf field.[24] Manipulating this three-level system by the microwave field and Raman lasers together may generate some interesting phenomena. Li *et al.*[25] discovered that electromagnetically induced transparency can be controlled by the relative phase between Raman lasers and the microwave field. Much more physics has been involved in the presence of both couplings.[26–28] Gain and loss can also be incorporated into coupled-two-level atoms, realizing two-energy-level systems with $\mathcal{PT}$ or anti-$\mathcal{PT}$ symmetry.[2,17,18,29–32] In addition, more energy levels may be designed to satisfy $\mathcal{PT}$ symmetry by lasers controlling, such as the interactions between lasers and a three-level or four-level atom.[33–36]

In this Letter, we theoretically study the dynamics of the $\mathcal{PT}$ symmetric two-level atoms in three regimes, i.e., unbroken $\mathcal{PT}$ symmetry, exception point (EP) and broken $\mathcal{PT}$ symmetry. We firstly study the time evolution of a Hermitian two-level system, then discuss eigenvalues, and finally investigate dynamics of the effective model with balanced gain and loss. We mainly focus on the effects of Rabi frequency and relative phase. Moreover, the effectively conserved two-level Hamiltonian is derived from the Λ-type model coupled with two optical fields and one rf field by means of adiabatically eliminating the third energy level.

We consider an effective two-level model with balanced gain and loss. The effective Hamiltonian can be derived from a Λ-type three-level system via adiabatic elimination of an excited state $|2\rangle$ under the large detuning condition (see Supplemental Material). The Hamiltonian is described as follows:

$$\begin{aligned} H_{\text{eff}} = & -i\gamma|1\rangle\langle 1| + (1-\Omega e^{i\phi})|1\rangle\langle 3| \\ & + i\gamma|3\rangle\langle 3| + (1-\Omega e^{-i\phi})|3\rangle\langle 1|, \end{aligned} \tag{1}$$

*Supported by the National Natural Science Foundation of China under Grant Nos 11104171, 11404199, 11574187 and 11604188, the Youth Science Foundation of Shanxi Province of China under Grant No 2012021003-1, and the Natural Science Foundation for Youths of Shanxi Province under Grant Nos 201601D201027 and 1331KSC.

**Corresponding author. Email: guolp@sxu.edu.cn

© 2018 Chinese Physical Society and IOP Publishing Ltd

where $(1-\Omega e^{\pm i\phi})$ describes the effective coupling between states $|1\rangle$ and $|3\rangle$, Ω is the effective strength of an rf field and atom, ϕ is the relative phase between rf and two laser fields, and γ is the amplitude of gain and loss.

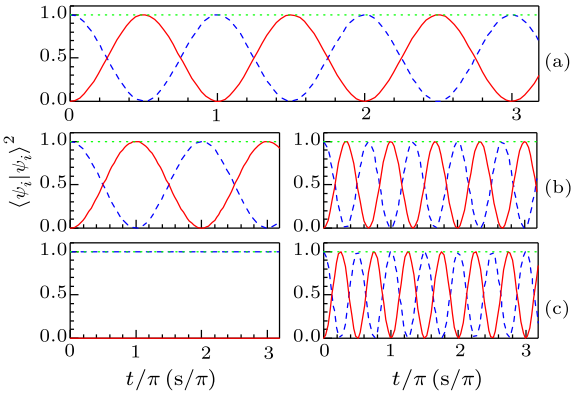

Fig. 1. Probability evolution of different values of Ω for $\gamma = 0$: (a) $\Omega = 0$; (b) $\Omega = 0.5$; and (c) $\Omega = 1.0$ with the left $\phi/2\pi = 0$ and the right $\phi/2\pi = 0.5$. The red solid line describes the density of $|3\rangle$; the blue dashed line describes the density of $|1\rangle$; and the green dotted line stands for the total density.

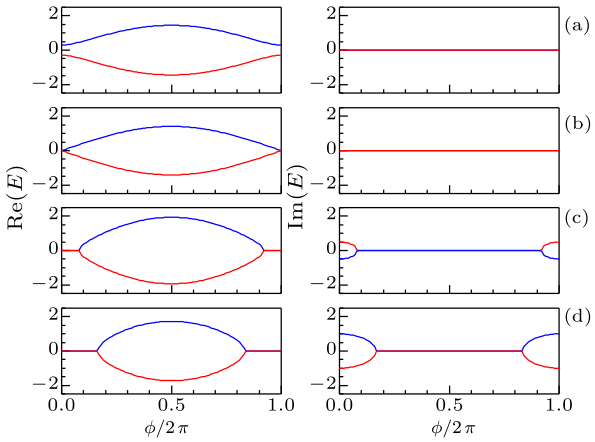

Fig. 2. Real (left) and imaginary (right) parts of the eigenvalues of the $\mathcal{PT}$-symmetric two-level system as a function of the relative phase $\phi/2\pi$: (a) $\Omega = 0.5$, $\gamma = 0.4$; (b) $\Omega = 0.5$, $\gamma = 0.5$; (c) $\Omega = 1.0$, $\gamma = 0.5$; and (d) $\Omega = 1.0$, $\gamma = 1.0$.

In the absence of γ, the system is a standard Hermitian case. The energy spectrum of the case is two branches, i.e., $E_\pm = \pm\sqrt{(1-2\Omega\cos\phi+\Omega^2)}$. For $\Omega < 1$, the two branches are well separated by the energy gap. When $\Omega = 1$, two branches touch at $\phi = 0$. When Ω is larger than 1, the energy gap opens again. The dynamics of the Hamiltonian (1) can be obtained by solving the corresponding Schrödinger equation

$$i\partial_t\psi = H_{\rm eff}\psi. \tag{2}$$

Considering the initial condition $\psi(t=0) = \psi_0$, the dynamic evolution equation can be integrated formally,

$$\psi(t) = \hat{U}(t)\psi_0,$$

where the time evolution operator is defined by $\hat{U}(t) = \exp(-iH_{\rm eff}t)$. We can analytically obtain

$$\hat{U}(t) = \begin{pmatrix} \cos(\omega_1 t) & -i\frac{(1-\Omega e^{i\phi})}{\omega_1}\sin(\omega_1 t) \\ -i\frac{(1-\Omega e^{-i\phi})}{\omega_1}\sin(\omega_1 t) & \cos(\omega_1 t) \end{pmatrix},$$

where $\omega_1 = |1-\Omega e^{i\phi}|$. As a specific example, we set the initial state as $\psi_0 = (1,0)^{\rm T}$. We can obtain the dynamics of both states at time t,

$$\begin{aligned} |\psi_1(t)|^2 &= \frac{1+\cos(2\omega_1 t)}{2}, \\ |\psi_3(t)|^2 &= \frac{1-\cos(2\omega_1 t)}{2}, \end{aligned} \tag{3}$$

where $|\psi_1(t)|^2$ ($|\psi_3(t)|^2$) is the occupation of $|1\rangle$ ($|3\rangle$). Figure 1 shows the probability evolutions of two states for different Ω following the Rabi oscillation with the periodicity π/ω_1. For $\Omega = 0$ and $\omega_1 = 1$, only the two-photon term determines the Rabi oscillation as shown in Fig. 1(a). With the increase of Ω and the relative phase $\phi = 0$ (the left column), the periodicity is larger than that in the case shown in Fig. 1(a). When $\Omega = 1$ and $\phi = 0$, the Rabi oscillation breaks down. The coexistence of rf-field and two optical fields coherently destructs the oscillation (the left panel of Fig. 1(c)). However, when $\phi = \pi$ the oscillation periodicity decreases with the increase of Ω as shown in the right column of Figs. 1(b) and 1(c). For the Hermitian case, we can see that the total occupation is always unit and time-independent.

In the presence of gain and loss ($\gamma \neq 0$), the eigenvalues of the $\mathcal{PT}$ symmetric Hamiltonian (1) are

$$E_\pm = \pm\sqrt{|1-\Omega e^{i\phi}|^2 - \gamma^2}. \tag{4}$$

Figure 2 describes the real and imaginary parts of the eigenvalues of the $\mathcal{PT}$-symmetric two-level system as a function of the relative phase ϕ for different Ω and γ. As shown in Fig. 2(b), when $\gamma = |1-\Omega e^{i\phi}|$, $E_+ = E_-$ and the eigenvectors coincide, which is defined as the EP $\gamma_{\rm PT}$. When $\gamma < \gamma_{\rm PT}$, the system has a purely real spectrum and satisfies the $\mathcal{PT}$ symmetry (Fig. 2(a)). However, when $\gamma > \gamma_{\rm PT}$, the eigenvalues are complex and the symmetry is spontaneously broken (Figs. 2(c) and 2(d)).

The dynamics of the non-Hermitian two-level quantum system can easily be calculated from the dynamic evolution Eq. (2). For the Hamiltonian (1) outside the EP, one obtains the evolution operator

$$\hat{U}(t) = \begin{pmatrix} \cos(\omega t) - \frac{\gamma}{\omega}\sin(\omega t) & -i\frac{1-\Omega e^{i\phi}}{\omega}\sin(\omega t) \\ -i\frac{1-\Omega e^{-i\phi}}{\omega}\sin(\omega t) & \cos(\omega t) + \frac{\gamma}{\omega}\sin(\omega t) \end{pmatrix}, \tag{5}$$

with the angular frequency

$$\omega = \sqrt{|1-\Omega e^{i\phi}|^2 - \gamma^2}. \tag{6}$$

When $\gamma = 0$, $\omega = \omega_1$. However, EPs ($\gamma = \gamma_{\rm PT}$) are singularities of the spectrum, at which spontaneous $\mathcal{PT}$ symmetry breaking has been observed in experiments.[3] It can lead to some new effects, e.g., chiral behavior and state-exchange process.[31,32] Hence, we also focus on the evolution of the system with the parameters approaching the EP, i.e., $\omega \to 0$. In this limit, the time evolution operator is

$$\hat{U}_{\rm EP}(t) \approx \begin{pmatrix} 1-\gamma t & -i(1-\Omega e^{i\phi})t \\ -i(1-\Omega e^{-i\phi})t & 1+\gamma t \end{pmatrix}. \quad (7)$$

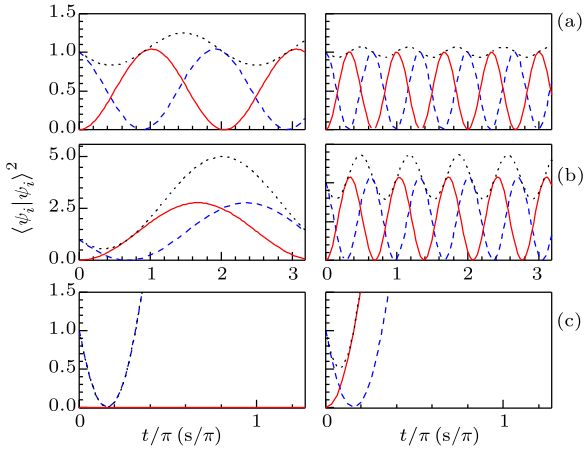

Fig. 3. The norm evolutions for non-Hermitian systems: $\phi = 0$ (left) and π (right). The first two rows with $\Omega = 0.5$ and two different values of γ: (a) $\gamma = 0.1$ and (b) $\gamma = 0.4$. The last row (c) $\Omega = 1.0$ and $\gamma = 2.0$. The red solid line describes the norm of $|3\rangle$, the blue dashed line is for the norm of $|1\rangle$, and the black dotted line is for the total norm.

For example, for an initial state $\psi_0 = (1,0)^{\rm T}$, we can find that outside the EP the norms of two levels are

$$|\psi_1(t)|^2 = \left|\cos(\omega t) - \gamma\frac{\sin(\omega t)}{\omega}\right|^2,$$
$$|\psi_3(t)|^2 = \left|i(1-\Omega e^{-i\phi})\frac{\sin(\omega t)}{\omega}\right|^2, \quad (8)$$

where $|\psi_{1,3}(t)|^2$ are the time-dependent periodic Rabi-type oscillation functions. The period π/ω is dependent on γ, Ω and ϕ, just as the depiction of Eq. (6). In detail, Fig. 3 describes some typical cases for the initial state in level $|1\rangle$. The left column depicts the dynamics for $\phi = 0$ and the right column for $\phi = \pi$. Simultaneously, the first two rows, Figs. 3(a) and 3(b), describe the dynamics of Eq. (1) with the same values of Ω and two different values of γ in the $\mathcal{PT}$-symmetric region ($\gamma < \gamma_{\rm PT}$), respectively. We can find that the envelope amplitudes increase with γ in the column direction. In addition, the corresponding periods of $\phi = 0$ are larger than that of $\phi = \pi$. The last row, Fig. 3(c), gives two cases when $\gamma \geqslant \gamma_{\rm PT}$. When $\Omega = 1$, $\phi = 0$ and $\gamma > \gamma_{\rm PT}$ (here $\gamma_{\rm PT} = 0$) due to the coexistence of rf-field and two optical fields coherently destructs only $|\psi_1(t)|^2$ first decreases and then increases to infinity, and meanwhile, $|\psi_3(t)|^2$ is zero all the time as shown in the left panel of Fig. 3(c). In fact, on the light side of Eq. (8) when $\Omega = 1$ and $\phi = 0$ $|\psi_3(t)|^2$ is always zero no matter whether γ is zero or not. When $\gamma = \gamma_{\rm PT}$ the wave function evolutes according to the operator Eq. (7) and the corresponding norms become

$$|\psi_1(t)|^2 = |1-\gamma t|^2,$$
$$|\psi_3(t)|^2 = |-i(1-\Omega e^{-i\phi})t|^2, \quad (9)$$

where $|\psi_1(t)|^2$ first decreases and then increases, and meanwhile, $|\psi_3(t)|^2$ increases always as shown in the right panel of Fig. 3(c). In a word, in the $\mathcal{PT}$ symmetric region, the time evolution of $|\psi_{1,3}(t)|^2$ is periodic Rabi-type oscillation, in the $\mathcal{PT}$ symmetric broken region the oscillations break down, and instead we observe an algebraic growth of the norms.

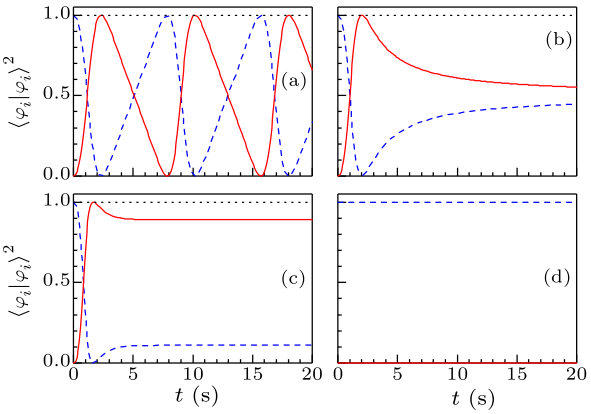

Fig. 4. The time evolutions of renormalized states for the initial state being $(1,0)^{\rm T}$ with $\Omega = 0.5$ and different values of γ: (a) $\gamma = 0.3$; (b) $\gamma = 0.5$; (c) $\gamma = 0.8$; and (d) $\gamma = 0.1$ and $\Omega = 1$. Here $\phi = 0$. The red solid line describes for φ_3, the blue dashed line describes the norm of φ_1, and the black dotted line is for the time-independent $|\varphi_1|^2 + |\varphi_3|^2$.

To compare with the Hermitian case, we normalize the total norm. The renormalized state vector[17,18] can be defined as

$$\varphi_j = \frac{\psi_j}{\sqrt{|\psi_1|^2 + |\psi_3|^2}}, \quad (10)$$

which satisfies $|\varphi_1|^2 + |\varphi_3|^2 = 1$ at any time. Then we deal with the time evolution of φ_j for the initial state being $(1,0)^{\rm T}$. Here $|\varphi_{1,3}(t)|^2$ are the Rabi-type oscillation in $\mathcal{PT}$ symmetric region (Fig. 4(a)). The evolution tends towards stability in $\mathcal{PT}$ symmetry broken regime as shown in Figs. 4(b) and 4(c). Figure 4(d) describes the dynamics similar to the left of Fig. 3(c). To better understand the underlying properties, according to the Hamiltonian (1) we consider the non-Hermitian effective Schrödinger equation

$$i\frac{d}{dt}\begin{pmatrix}\varphi_1\\ \varphi_3\end{pmatrix} = \begin{pmatrix} -i\gamma(1-\kappa) & 1-\Omega e^{i\phi} \\ 1-\Omega e^{-i\phi} & +i\gamma(1+\kappa)\end{pmatrix}\begin{pmatrix}\varphi_1\\ \varphi_3\end{pmatrix}, \quad (11)$$

where $\kappa = |\varphi_1|^2 - |\varphi_3|^2$. Further, in the familiar way

they are translated as the Bloch vectors

$$
\begin{aligned}
s_x &= \frac{1}{2}(\varphi_1^*\varphi_3 + \varphi_1\varphi_3^*),\\
s_y &= \frac{1}{2i}(\varphi_1^*\varphi_3 - \varphi_1\varphi_3^*),\\
s_z &= \frac{1}{2}(\varphi_1^*\varphi_1 - \varphi_3^*\varphi_3),
\end{aligned}
$$

which are always restricted on the surface of the Bloch sphere and satisfy $s_x^2 + s_y^2 + s_z^2 = 1/4$.[18] Then we can derive the generalized Bloch equations of motion from Eq. (11),

$$
\begin{aligned}
\dot{s}_x &= 4\gamma s_z s_x + 2\Omega s_z \sin\phi,\\
\dot{s}_y &= 4\gamma s_z s_y - 2(1 - \Omega\cos\phi)s_z,\\
\dot{s}_z &= -\gamma(1 - 4s_z^2) + 2s_y\\
&\quad - 2\Omega(s_y\cos\phi + s_x\sin\phi).
\end{aligned}
\tag{12}
$$

Thus we can obtain the effective Bloch dynamical evolution of this non-Hermitian system with different parameters by the fourth-order Runge–Kutta method. Figure 5 shows some typical examples of the effective Bloch dynamics for different values of γ, Ω and ϕ. When $\gamma < \gamma_{\rm PT}$, Fig. 5(a) shows that the evolution of the arbitrary initial state is the closed circle on the surface of the Bloch sphere, which surrounds either of the two fixed points (i),

$$
\begin{aligned}
s_x^0 &= \frac{-\Omega\gamma\sin\phi \pm \omega(1 - \Omega\cos\phi)}{2(1 - 2\Omega\cos\phi + \Omega^2)},\\
s_y^0 &= \frac{\gamma(1 - \Omega\cos\phi) \pm \omega\Omega\sin\phi}{2(1 - 2\Omega\cos\phi + \Omega^2)},\\
s_z^0 &= 0.
\end{aligned}
\tag{13}
$$

The fixed points are located in the x–y plane. Compared with the standard model in Ref. [18], we have more free parameters which are helpful to control dynamics. For example, with the change of Ω and ϕ, s_y^0 is not only positive, but also can take negative values. Even in the Hermitian case $\gamma = 0$, s_y^0 can take nonzero values due to the phase ϕ and Ω. However, at the EP, $\gamma = \gamma_{\rm PT}$, all initial states would evolute along the corresponding curves and turn back the only one fixed point (ii),

$$
\begin{aligned}
s_x^0 &= -\frac{\Omega\sin\phi}{2\gamma},\\
s_y^0 &= \frac{(1 - \Omega\cos\phi)}{2\gamma},\\
s_z^0 &= 0,
\end{aligned}
\tag{14}
$$

which are still located in the x–y plane as shown in Fig. 5(b). It is different from the only result $s_x^0 = 0$ mentioned in Ref. [18]. Figure 5(b) shows the effective Bloch dynamics for $\phi = 0$ or π, where the fixed point $s_x^0 = s_z^0 = 0$ and $s_y^0 = 1/2$. This helps to investigate the potential character at the EP. When the $\mathcal{PT}$ symmetry is broken ($\gamma > \gamma_{\rm PT}$), there are two fixed points again (iii),

$$
\begin{aligned}
s_x^0 &= -\frac{\Omega\sin\phi}{2\gamma},\\
s_y^0 &= \frac{(1 - \Omega\cos\phi)}{2\gamma},\\
s_z^0 &= \pm\frac{|\omega|}{2\gamma}.
\end{aligned}
\tag{15}
$$

The formulae of s_x^0 and s_y^0 are the same as Eq. (14), while they decrease with increasing γ. Compared with Eqs. (13) and (14), the z axis projections are no longer zero, which are labeled as $\pm$. Figure 5(c) shows any initial states on the Bloch sphere evolutes into one fixed point $(-)$, even if initial points are near the other one $(+)$. Thus the fixed point $(+)$ is defined as a source of the dynamics and the other $(-)$ is a sink of the dynamics. Figure 5(d) describes the dynamics of coherent subtraction, $\Omega = 1$ and $\phi = 0$, where the fixed points are $s_x^0 = s_y^0 = 0$ and $s_z^0 = \pm 1/2$, corresponding to the states $(1, 0)^{\rm T}$ and $(0, 1)^{\rm T}$. This is the reason why the evolution does not change with time (since the initial state mentioned above is $(1, 0)^{\rm T}$) as shown in the left panels of Figs. 3(c) and 4(d). In addition, the emergence of s_z^0 is the feature of the $\mathcal{PT}$ symmetry breaking. The fixed points are important for the dynamical evolution of $\mathcal{PT}$ symmetry systems.

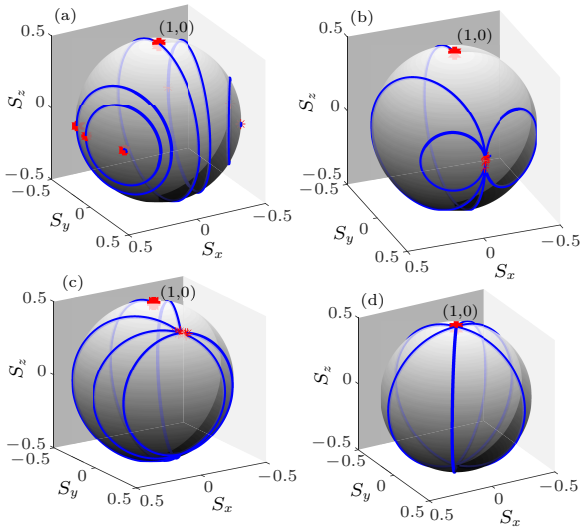

Fig. 5. Effective Bloch dynamics with the same parameters as in Fig. 4. Red asterisks * embody the initial state vectors of every evolution.

In summary, we have considered the effective two-level Hamiltonian with balanced gain and loss. When the system is conserved and Hermitian, the dynamical evolution performs Rabi oscillation and the oscillation periodicity can be controlled by the rf frequency and relative phase. There is one exception at which the rf field balances out the actions of two optical fields and oscillation is destructed. For the case of the effective two-level system with the $\mathcal{PT}$ symmetry, we study the dynamics in both regions of the unbroken and the broken $\mathcal{PT}$ symmetry at the EP.

Furthermore, using the renormalized state vector, the effective Bloch dynamical evolution has been studied under three conditions. Since the dynamics are closely related to the fixed points, we calculate the solutions under three-parameter conditions and find that the symmetry breaks when the z component of the fixed points is not zero, meanwhile the projection in the x–y plane can be fully adjusted by the phase and strength of optical and rf fields. The present results shall be helpful for the implementation of related experiments.

References

[1] Bender C M and Boettcher S 1998 *Phys. Rev. Lett.* **80** 5243
Bender C M, Boettcher S and Meisinger P N 1999 *J. Math. Phys.* **40** 2201
[2] Guo A, Salamo G J, Duchesne D, Morandotti R, Volatier-Ravat M, Aimez V, Siviloglou G A and Christodoulides D N 2009 *Phys. Rev. Lett.* **103** 093902
[3] Rüter C E, Makris K G, EI-Ganainy R, Christodoulides D N, Segev M and Kip D 2010 *Nat. Phys.* **6** 192
[4] Bittner S, Dietz B, Günther U, Harney H L, Miski-Oglu M, Richter A and Schäfer F 2012 *Phys. Rev. Lett.* **108** 024101
[5] Chang L, Jiang X, Hua S, Yang C, Wen J, Jiang L, Li G, Wang G and Xiao M 2014 *Nat. Photon.* **8** 524
[6] Feng L, Wong Z J, Ma R M, Wang Y and Zhang X 2014 *Science* **346** 972
[7] Hodaei H, Miri M A, Heinrich M, Christodoulides D N and Khajavikhan M 2014 *Science* **346** 975
[8] Hodaei H, Miri M A, Hassan A U, Hayenga W E, Heinrich M, Christodoulides D N and Khajavikhan M 2015 *Opt. Lett.* **40** 4955
[9] Schindler J, Lie A, Zheng M C, Ellis F M and Kottos T 2011 *Phys. Rev.* A **84** 040101
[10] Peng B, Ozdemir S K, Lei F, Monifi F, Gianfreda M, Long G L, Fan S, Nori F, Bender C M and Yang L 2014 *Nat. Phys.* **10** 394
Jing H, Özdemir S K, Geng Z, Zhang J, Lü X Y, Peng B, Yang L and Nori F 2015 *Sci. Rep.* **5** 9663
[11] Wimmer M, Miri M A, Christodoulides D and Peschel U 2016 *Sci. Rep.* **5** 17760
[12] Ben-Aryeh Y, Mann A and Yaakov I 2004 *J. Phys.* A **37** 12059
[13] Bender C M, Brody D C, Jones H F and Meister B K 2007 *Phys. Rev. Lett.* **98** 040403
[14] Graefe E M 2012 *J. Phys.* A **45** 444015
[15] Lian X, Zhong H, Xie Q, Zhou X, Wu Y and Liao W 2014 *Eur. Phys. J.* D **68** 189
[16] Baradaran M and Panahi H 2017 *Chin. Phys.* B **26** 060301
[17] Graefe E M, Korsch H J and Niederle A E 2008 *Phys. Rev. Lett.* **101** 150408
[18] Graefe E M, Korsch H J and Niederle A E 2010 *Phys. Rev.* A **82** 013629
[19] Zhu B G, Lü R and Chen S 2015 *Phys. Rev.* A **91** 042131
Zhu B G, Lü R and Chen S 2016 *Phys. Rev.* A **93** 032129
[20] Jin L and Song Z 2009 *Phys. Rev.* A **80** 052107
Yuce C 2015 *Phys. Lett.* A **379** 1213
Joglekar Y N, Scott D, Babbey M and Saxena A 2010 *Phys. Rev.* A **82** 030103(R)
[21] Bergmann K, Theuer H and Shore B W 1998 *Rev. Mod. Phys.* **70** 1003
[22] Alexanian M and Bose S K 1995 *Phys. Rev.* A **52** 2218
[23] Sun X L, Zhang J W, Cheng P F, Zuo Y N and Wang L J 2018 *Chin. Phys.* B **27** 023101
[24] Shahriar M S and Hemmer P R 1990 *Phys. Rev. Lett.* **65** 1865
[25] Li H, Sautenkov V A, Rostovtsev Y V, Welch G R, Hemmer P R and Scully M O 2009 *Phys. Rev.* A **80** 023820
[26] Luo B, Tang H and Guo H 2009 *J. Phys.* B **42** 235505
[27] Basler C, Grzesiak J and Helm H 2015 *Phys. Rev.* A **92** 013809
[28] Novikov S, Sweeney T, Robinson J E, Premaratne S P, Suri B, Wellstood F C and Palmer B S 2016 *Nat. Phys.* **12** 75
[29] Peng P, Cao W, Shen C, Qu W, Wen J, Jiang L and Xiao Y 2016 *Nat. Phys.* **12** 1139
[30] Bender C M, Brody D C and Jones H F 2002 *Phys. Rev. Lett.* **89** 270401
[31] Milburn T J, Doppler J, Holmes C A, Portolan S, Rotter S and Rabl P 2015 *Phys. Rev.* A **92** 052124
[32] Menke H, Klett M, Cartarius H, Main J and Wunner G 2016 *Phys. Rev.* A **93** 013401
[33] Hang C, Huang G and Konotop V V 2013 *Phys. Rev. Lett.* **110** 083604
[34] Li H, Dou J and Huang G 2013 *Opt. Express* **21** 32053
[35] Lee T E and Chan C K 2014 *Phys. Rev.* X **4** 041001
[36] Hao Y and Gu Q 2011 *Phys. Rev.* A **83** 043620

Supplemental Material: Dynamical evolution of an effective two-level system with $\mathcal{PT}$ symmetry

Lei Du(杜磊),[1] Zhihao Xu(徐志浩),[1,2,3] Chuanhao Yin(尹传昊),[4] and Liping Guo(郭利平)[1,2,3,*]

[1]*Institute of Theoretical Physics, Shanxi University, Taiyuan 030006, P. R. China*
[2]*Collaborative Innovation Center of Extreme Optics, Shanxi University, Taiyuan 030006, P.R.China*
[3]*State Key Laboratory of Quantum Optics and Quantum Optics Devices, Institute of Opto-Electronics, Shanxi University, Taiyuan 030006, P.R.China*
[4]*Institute of Physics, Chinese Academy of Sciences, Beijing 100080, P. R. China*

I. THE EFFECTIVE TWO-LEVEL HAMILTONIAN

To get the effective two-level Hamiltonian, we start from a Λ-type scheme shown in Fig. 1. Two hyperfine energy levels $|1\rangle$ and $|3\rangle$ are coupled by a rf-field. Simultaneously, two optical fields couple the hyperfine levels to an excited state $|2\rangle$ [1–4]. In the rotating frame of the two optical fields, the Hamiltonian is

$$\begin{aligned} H' = & \hbar\Delta_1 |1\rangle\langle 1| + \hbar\Delta_2 |3\rangle\langle 3| \\ & - \hbar\left(g|1\rangle\langle 2| + G|3\rangle\langle 2| + \Omega' e^{i\phi}|1\rangle\langle 3| + H.c.\right), \end{aligned} \tag{1}$$

where Δ_α ($\alpha = 1, 2$) are the detunings of the optical fields from the corresponding atomic resonances, g and G are Rabi frequencies of the two optical fields. Ω' is the coupling strength due to the rf-field, the phase ϕ can be controlled via the adjustment of the relative phase between the rf-field and two optical fields [1]. The dynamics of these three levels obeys the following Schrodinger equation,

$$i\hbar\partial_t |\psi(t)\rangle = H' |\psi(t)\rangle,$$

where the state $|\psi(t)\rangle$ is the superposition of three level states,

$$|\psi(t)\rangle = C_1(t)|1\rangle + C_2(t)|2\rangle + C_3(t)|3\rangle,$$

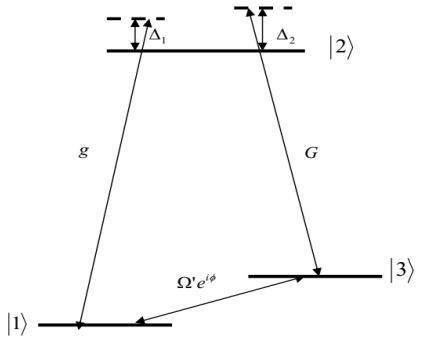

FIG. 1: Schematic illustration of three-level atomic system.

*Electronic address: guolp@sxu.edu.cn

with the coefficients $C_\alpha(t) \equiv \langle\psi|\alpha\rangle$ $(\alpha = 1, 2, 3)$. The equations of the coefficients are

$$\begin{aligned} i\partial_t C_1 &= (\Delta_1 - \Delta) C_1 - gC_2 - \Omega' e^{i\phi} C_3, \\ i\partial_t C_2 &= -\Delta C_2 - gC_1 - GC_3, \\ i\partial_t C_3 &= -\Omega' e^{-i\phi} C_1 - GC_2 + (\Delta_2 - \Delta) C_3, \end{aligned} \tag{2}$$

where all energies have already been translated by $-\hbar\Delta$, with $\Delta \equiv (\Delta_1 + \Delta_2)/2$. Since $|\Delta| \gg |\Delta_2 - \Delta_1|$ and $|\Delta| \gg \Gamma'$, where Γ' is the decay rate of $|2\rangle$, we can adiabatically eliminate C_2 from the dynamics of our system, $\partial_t C_2 = 0$ [6],

$$C_2 = -\frac{g}{\Delta} C_1 - \frac{G}{\Delta} C_3. \tag{3}$$

Substituting the equation (3) into (2), we obtain two coupled equations for the hyperfine states,

$$\begin{aligned} i\partial_t C_1 &= \left(\Delta_1 + \frac{g^2}{\Delta}\right) C_1 + \left(\frac{gG}{\Delta} - \Omega' e^{i\phi}\right) C_3, \\ i\partial_t C_3 &= \left(\frac{gG}{\Delta} - \Omega' e^{-i\phi}\right) C_1 + \left(\Delta_2 + \frac{G^2}{\Delta}\right) C_3. \end{aligned}$$

Hence, the effective Hamiltonian of the above equations is

$$\begin{aligned} H_{eff} = {} & \hbar\left(\Delta_1 + \frac{g^2}{\Delta}\right)|1\rangle\langle 1| + \hbar\left(\Delta_2 + \frac{G^2}{\Delta}\right)|3\rangle\langle 3| \\ & + \hbar\left(\frac{gG}{\Delta} - \Omega' e^{i\phi}\right)|1\rangle\langle 3| + \hbar\left(\frac{gG}{\Delta} - \Omega' e^{-i\phi}\right)|3\rangle\langle 1|. \end{aligned} \tag{4}$$

For simplicity, we set $g = G$, $\Delta_1 = \Delta_2 = \Delta$. The effective Hamiltonian can be shown as follows

$$H_{eff} = \begin{pmatrix} 0 & 1 - \Omega e^{i\phi} \\ 1 - \Omega e^{-i\phi} & 0 \end{pmatrix},$$

where the constant terms are neglected. Here $\hbar G^2/\Delta = 1$, then $\Omega = \Omega'\Delta/G^2$. The related experiments for Na [1] and Rb [2] atomic gases have been realized. In addition, the balanced loss or gain in our model can be realized by the control of decays into some one auxiliary state or vice versa [7].

[1] Shahriar M S and Hemmer P R 1990 Phys. Rev. Lett. **65**, 1865.
[2] Li H, Sautenkov V A, Rostovtsev Y V, Welch G R, Hemmer P R, and Scully M O 2009 Phys. Rev. A **80** 023820.
[3] Luo B, Tang H and Guo H 2009 J. Phys. B: At. Mol. Opt. Phys. **42** 235505.
[4] Basler C, Grzesiak J, and Helm H 2015 Phys. Rev. A **92** 013809.
[5] Rüter C E, Makris K G, EI-Ganainy R, Christodoulides D N, Segev M and Kip D 2010 Nature Phys. **6** 192.
[6] Steck D A 2006 *Quantum and Atom Optics,* available online at http://steck.us/teaching.
[7] Lee T E and Chan C-K 2014 Phys. Rev. X. **4**, 041001.